Influence of addition of organic fillers on the properties of mechanically recycled PLA

F.R. Beltrán[1,2], G. Gaspar[1], M. Dadras Chomachayi[3], A. Jalali-Arani[4], A.A. Lozano-Pérez[5], J.L. Cenis[5], M.U. de la Orden[2,6], E. Pérez[7], J. Martínez Urreaga[1,2]

[1] *Dpto. Ingeniería Química Industrial y Medio Ambiente, Universidad Politécnica de Madrid, E.T.S.I. Industriales, Madrid, 28006, Spain.*

[2] *Grupo de Investigación: Polímeros, Caracterización y Aplicaciones (POLCA)*

[3] *Mahshahr Campus, Amirkabir University of Technology, P.O. Box 63517-13178, Mahshahr, Iran*

[4] *Department of Polymer Engineering & Color Technology, Amirkabir University of Technology, P.O. Box 15875-4413, Tehran, Iran*

[5] *Dpto. Biotecnología, Instituto Murciano de Investigación y Desarrollo Agrario y Alimentario (IMIDA), Murcia, 30150, Spain*

[6] *Dpto. de Química Orgánica I, Universidad Complutense de Madrid, Facultad de Óptica y Optometría, Madrid, 28037, Spain*

[7] *Instituto de Ciencia y Tecnología de Polímeros, CSIC, 28006, Madrid*

Abstract

Poly(lactic acid) (PLA) is one of the most used biobased and biodegradable polymers. Due to their high stability, some of the newest grades of PLA are only degradable under severe industrial conditions. For these grades, mechanical recycling is a viable end-of-life option, with great environmental advantages. However, the polymer undergoes degradation during its service life and in the melt reprocessing, which leads to a decrease in properties that can compromise the demand for recycled plastic. The goal of this work was to evaluate the usefulness of adding small amounts of two organic fillers, during the recycling process, for improving the properties of the recycled plastic. The two organic fillers, chitosan and silk fibroin nanoparticles, are obtained from renewable resources. The behavior of the recycled plastics depends on the degradation level of the aged polymer and the nature and amount of the organic filler added. The fillers reduce the further degradation during the melt reprocessing of PLA previously subjected to severe hydrolysis, thus increasing the intrinsic viscosity of the recycled plastic. A careful selection of the organic filler added, based on the nature of the aged plastic, lead to recycled plastics with significant improvements in key mechanical, thermal and barrier properties. Thus, the use of organic fillers obtained from renewable resources can be the basis of a cost-effective and environmentally sound way for improving the mechanical recycling of plastics such as PLA.

Keywords

Poly(lactic acid); mechanical recycling; silk fibroin; chitosan; gas barrier properties

Acknowledgements

The authors would like to thank the Institute of Polymer Science and Technology (Madrid, Spain), for collaborating in the SEM measurements. This work was supported by MINECO-Spain (project CTM2017-88989-P), Universidad Politécnica de Madrid (project UPM RP 160543006) and the European Comission (Horizon 2020, project 860407-BIO-PLASTICS EUROPE).

1. Introduction

In recent years, the environmental problem generated due to the massive utilization of fossil-fuel based plastics, and the inadequate management of such wastes, has raised a fair amount of attention. Among the most important solutions posed to this problem is the progressive substitution of fossil-based plastics, in certain applications, with bioplastics such as poly(lactic acid) (PLA). PLA is an aliphatic polyester, produced via ring opening polymerization of lactide, a dimer of lactic acid obtained from the fermentation of carbohydrates present in corn, sugar cane or potato (Castro-Aguirre et al., 2016). PLA is one of the most researched and used bioplastics, due to its biodegradability, biocompatibility and acceptable mechanical and optical properties (Farah et al., 2016, Reddy et al., 2013). The production, and consumption, of PLA has grown steadily over the last years, exceeding the 200 kt in 2018 (Chinthapalli et al., 2019). Such increase could be attributed to the development of new grades with improved properties (Nagarajan et al., 2016), which allow the utilization of PLA in a wide range of applications such as food packaging and textile industry (Cecchi et al., 2019).

The utilization of PLA in applications typically related to fossil-fuel based polymers leads to the reduction of the consumption of non-renewable feedstocks. However, PLA grades destined to demanding applications degrade at a very low rate and are compostable only in industrial conditions (Haider et al., 2018, Niaounakis, 2019), which, in conjunction with an inadequate management of the wastes, could result in an important environmental problem. Furthermore, it cannot be ignored that the production of the feedstock used in the manufacture of PLA requires large amounts of croplands, which might end resulting in food supply and overpricing issues, especially in poorer countries (Mülhaupt, 2013). Therefore, the development of environmentally friendly methods for the management of PLA wastes is crucial in the sustainability of this bioplastic. Among the potential valorization methods, mechanical recycling plays a prominent role, since several Life Cycle Assessment studies point out that it allows to reduce the environmental impact by decreasing the consumption of raw materials and emissions (Rossi et al., 2015, Soroudi and Jakubowicz, 2013, Zhao et al., 2018).

Despite the environmental advantages of the mechanical recycling of PLA, a holistic approach of the recycling process is necessary to assure its feasibility. On the one hand, plastic recovery infrastructures should be adapted to allow the introduction of a separate stream for PLA. On the other hand, previous studies indicate that some crucial properties in packaging applications decrease during the mechanical recycling of the plastic (Beltrán et al., 2018a), which might negatively affect the market for the recycled PLA, and thus threaten the sustainability of the process . Consequently, it is necessary to develop economical and environmentally friendly methods that allow to improve the

performance of recycled PLA, increasing its attractive to the plastic transformers. It has been reported in previous works that the use of additives during the mechanical recycling, such as functionalized clays (Beltrán et al., 2018c) or chain extenders and crosslinking agents (Beltrán et al., 2019), allow to reduce the degradation of the polymer, thus improving the properties of the recycled material.

Another potential alternative for improving the properties of recycled PLA is the utilization of organic fillers coming from renewable resources. This kind of fillers are very interesting due to their low cost, availability and biodegradability. For example, Tesfaye et al. reported that silk fibroin nanocrystals have a nucleating effect on PLA, and also help to reduce the reduction of the intrinsic viscosity during multiple reprocessing cycles (Tesfaye et al., 2017). In the same line, Patwa et al. reported that the addition of silk nano-discs to PLA led to an increase in crystallization and improvements in thermal stability, toughness and gas barrier properties (Patwa et al., 2018). Other authors, such as Li et al. have added small amounts of functionalized chitosan to PLA, obtaining improvements on the Young modulus and tensile strength of the polymer (Li et al., 2019).

The previously mentioned studies point out that is possible to use organic filler to improve the properties of PLA. However, there is very little data regarding the effect of organic fillers, concretely silk fibroin nanoparticles (SFN) and chitosan, on the structure and properties of post-consumer PLA subjected to mechanical recycling. Consequently, the main aim of this work is to study the effects of different organic fillers on the structure and thermal, mechanical, gas barrier and optical properties of mechanically recycled PLA. In order to simulate the polymer degradation during its service life, two accelerated ageing processes were carried out. A simulated post-consumer PLA was obtained by subjecting neat PLA to (i) a melt compounding and compression-molding step, (ii) an accelerated ageing process comprising hydrothermal and photochemical degradation steps, and (iii) a demanding washing step. In a parallel way, severely degraded PLA was obtained by hydrolytic degradation of neat PLA at 60 ºC for 5 days. Then, both post-consumer and hydrolyzed PLA were melt compounded along with the SFN and chitosan, compressed molded into films and characterized by solution viscosimetry, microhardness measurements, differential scanning calorimetry (DSC), thermogravimetric analysis (TGA) and gas permeability and water vapor transmission rate (WVTR) measurements.

2. Materials and methods

2.1. Materials

Ingeo™ 2003D, a commercial grade of PLA with a a melt mass-flow rate of 6 g/10 min (2.16 kg at 210 ºC) was used. *Bombyx mori* silkworm cocoons were obtained from the University of Guilan (Iran) and from IMIDA (Spain). The ionic liquid (IL) 1-ethyl-3-methylimidazolium acetate (95 % purity) was purchased from IoliTec GmbH. Sodium carbonate (Na_2CO_3) and chloroform were purchased from Merck. Sulfuric acid (96 % purity) was supplied by Honeywell. High molecular weight chitosan (HCh, M_w 100-300 kDa) was supplied by Acros Organics, and low molecular weight chitosan (LCh, M_v 50-150 kDa) was supplied by Sigma Aldrich.

2.2. Preparation of silk fibroin nanoparticles (SFN)

Bombyx mori cocoons were boiled twice for 30 min in an aqueous solution of Na_2CO_3 (0.5 % w/v) at 98 °C, followed by washing several times with distilled water to remove impurities and sericin. After the degumming step, silk fibroin nanoparticles were prepared using two different methods. In one process, the degummed silk fibroin (SF) was dried overnight at 50 °C, and then hydrolyzed in an aqueous solution of H_2SO_4 (64 wt. %) at 45 °C under continuous stirring. The reaction was stopped by adding 50 ml of distilled water after 2 h. The mixture was then centrifuged at 5,000 rpm for 15 min to reach a neutral pH. Finally, the silk fibroin hydrolysate was dialyzed in a cellulose membrane tube (molecular weight cut-off 3.5 kD) against distilled water for 4 days and freeze-dried, for 48 h, to obtain the dry SFN (HSFN).

The second process is based in the work of Lozano-Pérez et al. (Lozano-Pérez et al., 2015). In this process, a degummed SF-IL solution (10 wt. %) was prepared using a Branson 450D sonicator (30 % amplitude) at 90 ºC. Then, 3 mL of water were added to the solution and the mixture was heated to 60 ºC. The solution was sprayed onto 100 mL of stirred methanol at 20 ºC. The resulting white suspension was stirred for 2 h at room temperature and then centrifuged (13400 rpm for 15 mins, at 4 ºC). The supernatant was then removed, and fresh methanol was added to the precipitate and mixed using a vortex mixer (2 min) and a sonicator (5 min). The resulting suspension was centrifuged again in the same conditions. Finally, the white precipitate was washed with water and freeze-dried for 72 h to obtain the SFN (ILSFN).

2.3. Preparation of the samples

Scheme 1 summarizes the process followed for the ageing of PLA and subsequent preparation of the recycled PLA-based materials. Two different ageing processes were used to consider different levels of degradation in PLA wastes. In the first process, a simulated post-consumer PLA was obtained by subjecting neat PLA to an extrusion process in a Rondol Microlab twin-screw extruder (L/D = 20), at 60 rpm and with a temperature profile from hopper to die: 125, 160, 190, 190, 180 ºC. The obtained material was compressed molded into films (200 ± 10 µm) at 190 ºC, using an IQAP-LAP hot plate press. The films (PLAV) were then subjected to an accelerated ageing comprising 40 h of photochemical degradation in an Atlas UVCON chamber, equipped with eight F40UVB lamps; 468 h of thermal degradation at 50 ºC in an oven and 240 h of hydrolytic degradation at 25 ºC in demineralized water. Finally, the aged material was washed for 15 min, at 85 ºC in an aqueous solution of NaOH (1.0 % wt.) and a surfactant (Triton X, 0.3 % wt.), as it has been suggested in previous studies (Beltrán et al., 2019). In the second process, neat PLA was immersed in demineralized water at 60 ºC for five days to obtain a severely degraded PLA (hydrolyzed PLA).

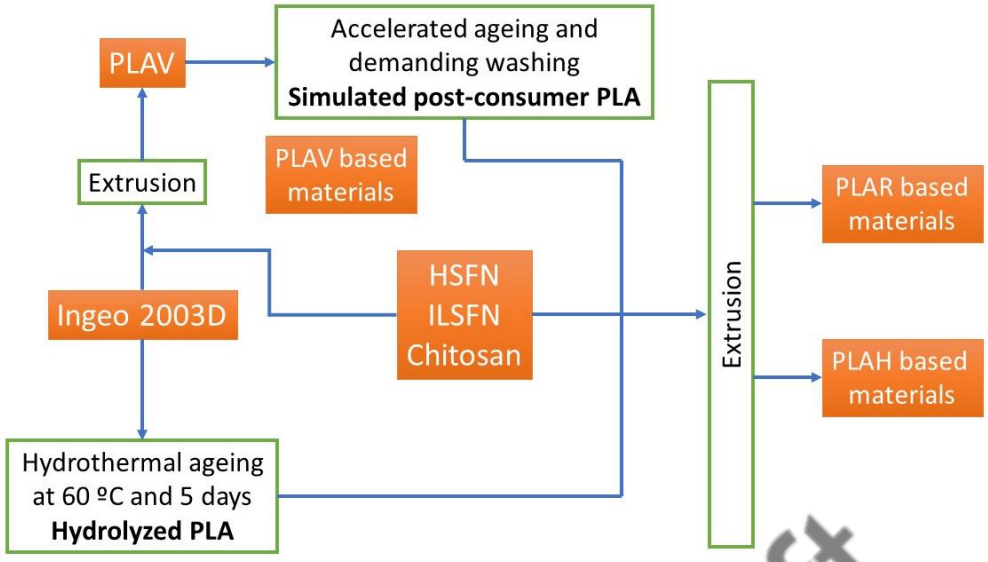

Scheme 1. Preparation of the different samples.

After the different ageing processes, both hydrolyzed and post-consumer PLA were extruded in conjunction with four different organic fillers: HSFN, ILSFN and chitosan (high and low molecular weight). The nanoparticles were added in a proportion of 1 % wt., while the chitosan was added in a proportion of 1 and 5 % wt. Lastly, the recycled materials were transformed into films (200 ± 10 µm) by compression molding. The obtained materials are summarized in table 1

Table 1. Materials obtained after the recycling process

Sample	Description
PLAV	PLA subjected to the first extrusion and compression molding step
PLAR	Simulated post-consumer PLA, subjected to a second extrusion and compression molding step
PLAH	Hydrolyzed PLA, subjected to an extrusion and compression molding step
PLAR-1HSFN	PLAR with 1% of silk fibroin nanoparticles obtained via hydrolysis
PLAH-1HSFN	PLAH with 1% of silk fibroin nanoparticles obtained via hydrolysis
PLAR-1ILSFN	PLAR with 1% of silk fibroin nanoparticles obtained via ionic liquid dissolution
PLAR-2ILSFN	PLAR with 2% of silk fibroin nanoparticles obtained via ionic liquid dissolution
PLAH-1ILSFN	PLAH with 1% of silk fibroin nanoparticles obtained via ionic liquid dissolution
PLAR-1LCh	PLAR with 1% of low molecular weight chitosan
PLAR-5LCh	PLAR with 5% of low molecular weight chitosan
PLAH-1LCh	PLAH with 1% of low molecular weight chitosan
PLAH-5LCh	PLAH with 5% of low molecular weight chitosan
PLAR-1HCh	PLAR with 1% of high molecular weight chitosan

PLAR-5HCh	PLAR with 5% of high molecular weight chitosan

2.4. Characterization techniques

Intrinsic viscosity of the different materials was measured using an Ubbelohde viscometer, at 25 ºC, using chloroform as a solvent. The measurements were made at four different concentrations.

A Type M Shimadzu microhardness tester was used to measure the Vickers hardness of the different samples. A Vickers pyramidal indenter was used to apply a load of 25 g during 10 s. Each sample was measured six times.

Fourier-transform infrared (FTIR) spectra of the different samples were recorded with a Nicolet iS10 spectrometer, equipped with a diamond Attenuated Total Reflectance (ATR) accessory. 16 scans and a 4 cm^{-1} resolution were used.

Differential scanning calorimetry (DSC) scans of the different materials were performed in a TA Instruments Q20 calorimeter, under nitrogen atmosphere (50 mL/min). Samples of 5 mg were placed in aluminum pans, heated from 0 to 180 ºC and kept at 180 ºC for 3 minutes. Subsequently, the samples were cooled to 0 ºC, kept at 0 ºC for 1 minute and, finally, heated again to 180 ºC. All the scans were performed at a heating or cooling rate of 5 ºC/min.

The thermal stability of the samples was studied by means of thermogravimetric analysis (TGA), which was conducted in a TA Instruments TGA2050 thermobalance, using 10 mg samples, under nitrogen atmosphere (30 mL/min). The samples were heated from room temperature to 800 ºC at 10 ºC/min.

The permeability against oxygen and was measured in a homemade permeation cell, at 30 ºC and with a gas pressure of 1 bar. The water vapor transmission rate (WVTR) of the different samples was measured according to the ISO 2528 standard. Thin films (9 ± 2 µm) of the different materials were prepared by casting (0,1 g of polymer/ml of chloroform). The permeability cups were filled with 2 g of dry silica gel, sealed with the sample film and placed in a 90 % relative humidity atmosphere at 23 ºC. The cups were weighed after different exposure times. *WVTR* (g/day·cm^2) was determined using equation 1:

$$WVTR = \frac{240*(m_t - m_0)}{A*t} \quad (1)$$

where m_t is the mass of the cup at time $_t$, m_0 is the initial mass of the cup and $_A$ is the exposed area of the film. Each sample was measured three times.

3. Results and discussion

3.1. Morphology of the PLA based materials

(a)

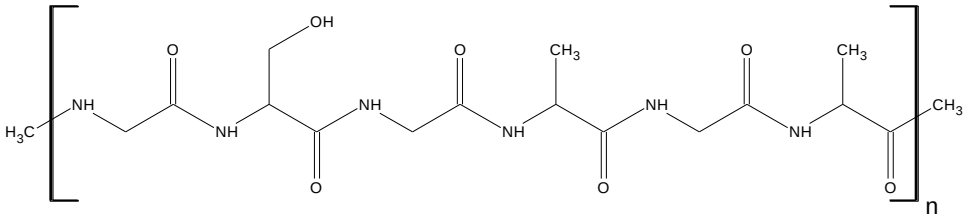

(b)

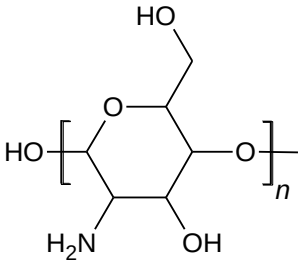

Figure 1. Chemical structures of (a) silk fibroin and (b) chitosan

The filler dispersion plays a prominent role in key properties of PLA based materials, such as intrinsic viscosity, hardness and gas barrier properties. Therefore, it is important to determine the dispersion of the different organic fillers, in order to obtain recycled materials with improved properties, and thus, more attractive to the plastics market. The dispersion of the different fillers in the PLA matrix was studied using scanning electron microscopy. Figures 2a-d correspond to the different PLA samples filled with HSFN and ILSFN. Overall, silk fibroin nanoparticles (diameter < 500 nm) show a good dispersion in the PLA matrix. This behavior could be attributed to the hydrophobic character of the silk fibroin, which increases the compatibility with an hydrophobic matrix, such as PLA, thus facilitating the dispersion of the nanoparticles (Patwa et al., 2018, Tesfaye et al., 2017). Furthermore the -NH and -OH groups present in the structure of SFN (figure 1) might interact with the terminal -COOH and -OH groups present in both post-consumer and hydrolyzed PLA (Beltrán et al., 2018b), improving the compatibility between both materials. However, some aggregates bigger than 1 µm were observed, especially in the samples with ILSFN (figure 2d). To better understand this behavior, it is necessary to analyze the chemical structure of the nanoparticles by means of FTIR-ATR.

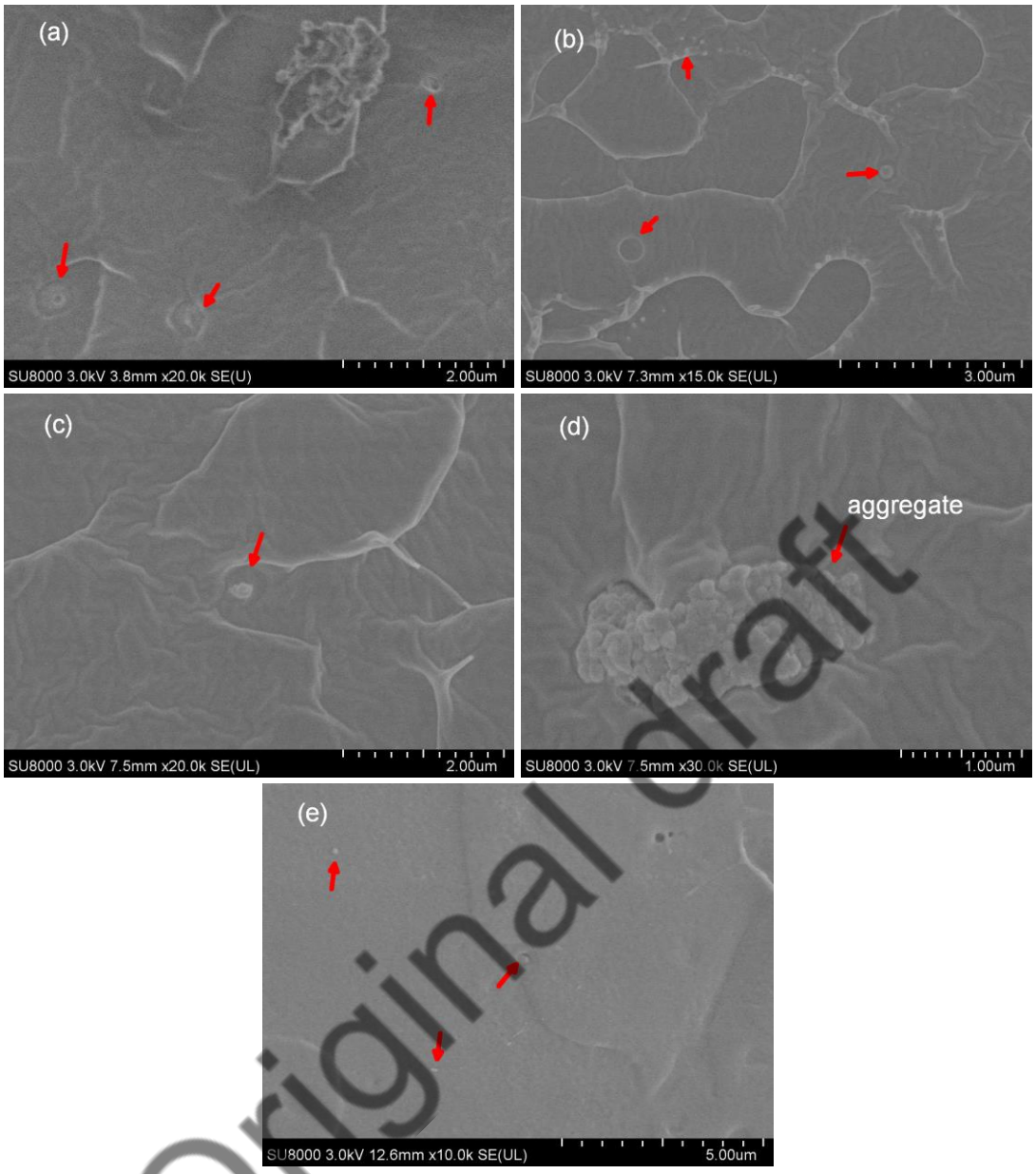

Figure 2. SEM photographs of (a) PLAR-1HSFN, (b) PLAH-1HSFN, (c) and (d) PLAR-2ILSFN and (e) PLAR-5HCh.

Figure 3 shows the FTIR-ATR spectra of both HSFN and ILSFN. As it could be expected, the spectra of both samples are very similar, showing the typical absorption bands around 1630, 1520 and 1230 cm^{-1} that correspond to amide I, amide II and amide III, respectively. However, it is worth to note that there are some slight differences between the spectra of both nanoparticles. In ILSFN, the amide I band is displaced toward lower wavenumbers and the amide III band shows a small shoulder at 1267 cm^{-1}. Both changes are related to the transformation from a random coil structure, named silk I, to a better organized sheet structure known as silk II (Tao et al., 2012, Tesfaye et al., 2017). The presence of a more ordered structure might result in stronger molecular interactions inside the ILSFN nanoparticles via hydrogen bonding between the -NH and -OH groups

present in the structure of silk fibroin (figure 1). Such interactions favor the formation of aggregates and result in a poorer dispersion of the ILSFN in the PLA matrix.

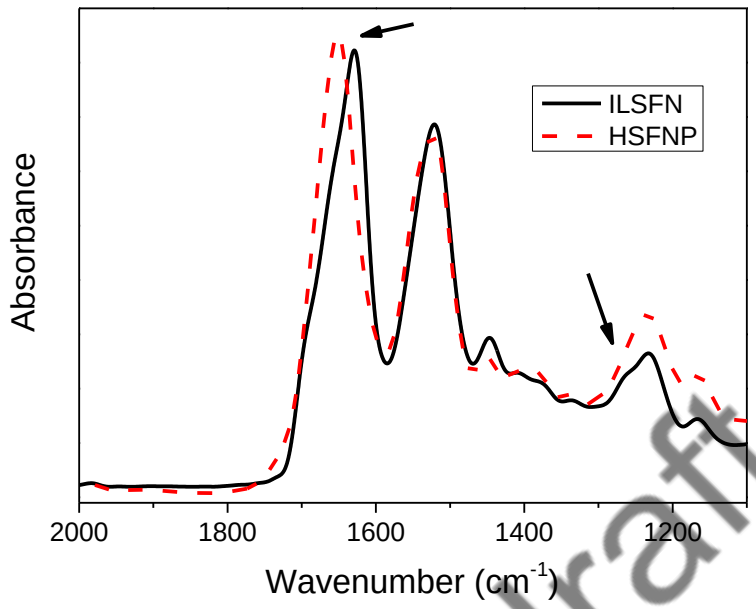

Figure 3. FTIR-ATR spectra of the HSFN and ILSFN.

Regarding the behavior of the samples with chitosan, previous studies conducted by Li et al. (Li et al., 2019) and Suyatma et al. (Suyatma et al., 2004) point out that PLA and chitosan are immiscible, due to the hydrophilic nature of chitosan. Figure 2e shows that, despite there are some holes that indicate poor adhesion between phases, the dispersion of the high molecular chitosan is relatively good. To explain this behavior, one should consider the presence of carboxyl and hydroxyl end groups in recycled PLA. These groups might interact with the hydroxyl and amino groups present in chitosan (figure 1), thus improving the compatibility between the two polymeric phases.

3.2. Properties of the PLA based materials

3.2.1. Intrinsic viscosity of the PLA based materials

The intrinsic viscosity is one of the most important properties of plastics such as PLA and other polyesters, not only because of its relationship with molecular weight, but for the role it plays on the processing of the plastics. The industrial manufacturing processes are designed to operate at specific conditions, thus, drastic changes in the intrinsic viscosity of recycled PLA might discourage the use of this plastic. The effect of the organic fillers on the intrinsic viscosity of PLA was measured by means of solution viscosimetry and the results are presented in figure 4. It can be seen that the accelerated ageing, washing and reprocessing lead to a decrease of approximately 13 % of the intrinsic viscosity of PLA. This phenomenon was previously studied (Beltrán et al., 2018b) and it can be attributed to the degradation processes that take place during the whole recycling process. Several chain scission mechanisms are involved in the

degradation of PLA during recycling, such as hydrolysis, oxidative random chain scission and inter and intra-molecular transesterification (Cuadri and Martín-Alfonso, 2018). PLAH presents a much lower intrinsic viscosity, less than 50% of the virgin polymer viscosity, thus showing the massive chain scission caused by the severe hydrolytic degradation to which the polymer was subjected.

Regarding the behavior of the samples filled with silk fibroin nanoparticles, figure 4 shows that effect varies with both the type of nanoparticle and the level of degradation of PLA. For PLAR, the recycled polymer obtained from slightly degraded PLA, the nanoparticles obtained via acid hydrolysis seem to cause the degradation of PLA, while those obtained by dissolution in ionic liquids do not significantly affect the intrinsic viscosity of the polymer. Tesfaye et al. (Tesfaye et al., 2017) and Patwa et al. (Patwa et al., 2018) reported a similar behavior in samples of PLA and silk fibroin nanoparticles obtained via acid hydrolysis. This behavior could be explained considering the presence of some residual acid groups in the nanoparticles, since it is known that acid groups can catalyze the degradation of PLA during melt processing (Auras et al., 2010). The different behavior of ILSFN could be due to that this fibroin was obtained in the absence of sulfuric acid and to the poor interaction between PLA and ILSFN, as it was seen by means of SEM microscopy.

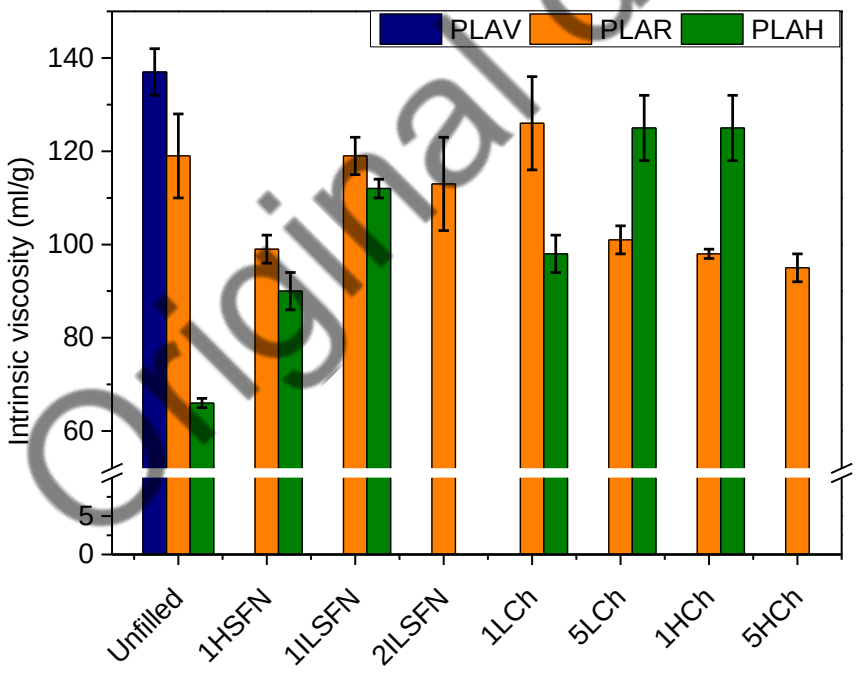

Figure 4. Intrinsic viscosity of the PLA based materials.

Figure 4 also shows that the PLAH samples containing silk fibroin present a different behavior than those of PLAR. In PLAH based materials the addition of both HSFN and ILSFN led to important increases of the intrinsic viscosity, which could expand the applications of the recycled plastic. These results are rather surprising, since the presence of HSFN can catalyze the degradation of PLA during processing, as it has

been shown above. However, it must be taken into account that, due of the severe hydrolytic degradation suffered, PLA has a large amount of terminal -COOH groups, which catalyze the subsequent degradation of PLA during the melt reprocessing step to obtain PLAH. The presence of fibroin nanoparticles during the reprocessing step could block, through acid-base interactions, a significant proportion of such –COOH groups, thus limiting their pernicious catalytic effect. Patwa et al. also observed that silk fibroin can limit the degradation of PLA during processing (Patwa et al., 2018). These authors pointed out that, in certain conditions, PLA and SFN could interact and form structures that delay the chain movement during processing, thus contributing to decrease the degradation of the polymer.

The positive effect of the fibroin depends on the process of obtaining the nanoparticles. Again, the material reinforced with fibroin nanoparticles obtained by acid hydrolysis show lower intrinsic viscosity, probably due to the presence of some acid groups that catalyze the polymer degradation during the melt reprocessing.

Regarding the behavior of the samples with chitosan, figure 4 shows that the level of degradation of PLA and the molecular weight of chitosan play a very important role on the final intrinsic viscosity of the materials. The PLAR-1LCh sample presents no significant change of the intrinsic viscosity, while the rest of the PLAR-chitosan materials show lower values in comparison with PLAR (around 18%). The behavior of PLAR-1LCh could be explained by the low amount of chitosan and the poor interaction between PLA and this kind of chitosan. However, the reduced viscosity observed in the other composites of PLA and chitosan has not been fully explained, although Hijazi et al. (Hijazi et al., 2019) reported that higher amounts of chitosan nanoparticles could contribute to increase the shear stresses during the extrusion, resulting in further degradation of PLA.

The behavior of the PLAH samples is very different. The addition of chitosan led in these cases to an increase of the intrinsic viscosity, regardless of the concentration and molecular weight, as opposed to the PLAR samples. As it was discussed for the PLAH samples reinforced with fibroin nanoparticles, this behavior could be due to the high amount of terminal -COOH groups present in the severely hydrolyzed PLA. The amino groups present in the structure of chitosan (Figure 1) can block some of such terminal -COOH groups (Elsawy et al., 2017), thus reducing their catalytic effect on the degradation of the polymer during melt reprocessing. A similar effect was obtained in a previous work by using amino-modified halloysite in the recycling of PLA (Beltrán et al., 2018c).

3.2.2. Thermal properties of the PLA based materials

The properties, and hence the applications, of the recycled plastics depend on the thermal transitions and crystalline structures of the polymer. The effects of the different organic fillers on the thermal behavior of PLA, studied by means of DSC,are summarized on figure 5 and table 2. It can be seen on figure 5a that virgin PLA show a glass transition close to 60 ºC, an exothermic peak corresponding to cold crystallization, between 105 and 110 ºC, and a double melting endothermic peak over 140 ºC. The presence of this double melting behavior has been reported in previous studies (Beltrán et al., 2018b, Di

Lorenzo, 2006), and is related to a melt recrystallization mechanism in which less perfect crystals melt at lower temperatures, rearrange into more ordered structures and melt at higher temperatures. The mechanical recycling causes some differences in the thermal transitions of PLA. Firstly, it can be seen on both figure 5a and table 2 that recycled PLA has a lower cold crystallization temperature (T_{cc}) value than PLAV. This behavior could be attributed to the degradation of the polymer during the ageing, washing and reprocessing processes, since shorter polymer chains crystallize more easily. Secondly, it can be seen that the high temperature melting peak is more relevant in the recycled polymer, which can also be related to the presence of shorter polymer chains. The shorter polymer chains have increased mobility and can rearrange more easily into more perfect structures (Beltrán et al., 2016).

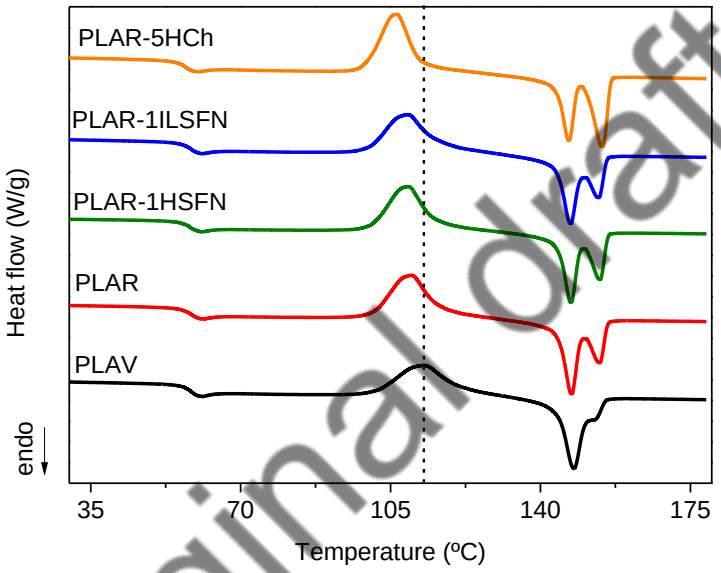

Figure 5. DSC second heating scans of the PLA based materials.

Regarding the behavior of the samples with organic fillers, Figure 5 and table 2 show that the use of organic nanofillers in the recycling process cause small displacements of T_{cc} towards lower values. This displacement, although is small, could be an indicative of the nucleating effect of the nanoparticles on the crystallization of PLA. This result is in good agreement with those reported by other authors for virgin PLA reinforced with fibroin nanoparticles (Tesfaye et al., 2017) and chitosan (Elsawy et al., 2016). However, the small differences observed in table 2 in the values of T_{cc}, ΔH_{cc} and ΔH_m, point out that the nucleating effect of the organic nanoparticles is limited.

Table 2. DSC results (second heating scan) of the PLA based materials.

Sample	T_g (ºC)	T_{cc} (ºC)	T_m (ºC)	ΔH_{cc} (J/g)	ΔH_m (J/g)
PLAV	58.4	112.8	147.8	25.2	26.6
PLAR	58.5	109.9	147.3 - 153.0	28.2	28.7
PLAH	56.8	106.1	146.3 - 154.3	33.3	36.2

PLAR-1HSFN	58.1	109.1	147.2 - 153.9	27.0	28.0
PLAH-1HSFN	57.7	104.4	146.5 - 154.7	32.2	33.4
PLAR-1ILSFN	58.4	109.0	147.1 - 153.7	27.4	28.2
PLAR-2ILSFN	58.4	107.6	147.0 - 154.0	26.8	27.6
PLAH-1ILSFN	57.7	104.4	146.5 - 154.7	32.2	33.4
PLAR-1LCh	58.5	109.1	147.2 - 153.5	25.3	25.9
PLAR-5LCh	57.7	107.7	146.6 - 154.2	29.4	29.8
PLAH-1LCh	57.6	106.7	146.4 - 154.4	32.2	35.0
PLAH-5LCh	57.8	107.5	146.7 - 154.7	28.3	30.2
PLAR-1HCh	58.4	106.3	146.6 - 154.2	29.2	29.4
PLAR-5HCh	57.2	106.6	146.7 - 154.4	31.1	31.5
PLAH-1HCh	57.6	107.5	146.8 - 154.6	31.4	32.2

Table 3 summarizes the TGA characteristic temperatures of the different PLA samples. T_{10} and T_{max} correspond to the temperature at which 10 % of the mass is loss and the temperature of maximum degradation rate, respectively, and are commonly used an indicator of the thermal stability of the materials. Table 3 shows that mechanical recycling causes a decrease of the thermal stability of PLA. This result has been reported in previous studies, and its related to the degradation of PLA during the ageing and recycling processes (Beltrán et al., 2018b). The samples with lower molecular weight have shorter polymer chains, which decompose at lower temperatures, negatively affecting the thermal stability. The presence of the fibroin nanoparticles is positive, because they lead to slight increases in the thermal stability of the recycled plastic, especially in PLAR. To understand this behavior, one should consider the barrier effect of the nanoparticles dispersed in the polymer matrix, which hinder the liberation of the decomposition products and increase the thermal stability of the samples. Furthermore, Patwa et al. (Patwa et al., 2018) reported that SFN restrict the thermal motion of the polymer chains. Finally, table 3 shows that all the PLAR-chitosan samples, with the exception of PLAR-1LCh, have a lower thermal stability than PLAR. These results could be explained by the variations of the molecular weight observed by means of intrinsic viscosity measurements. Regarding the PLAH-chitosan samples, the effect of the low molecular weight chitosan on the thermal stability of PLA is relatively small, while the high molecular chitosan caused a decrease of the thermal stability of the sample.

Table 3. TGA characteristic temperatures of PLA based materials.

Sample	**T_{10} (ºC)**	**T_{max} (ºC)**
PLAV	335.4	369.1
PLAR	327.6	367.5
PLAH	325.9	364.5
PLAR-1HSFN	334.3	367.0
PLAH-1HSFN	325.1	361.4
PLAR-1ILSFN	331.5	370.1
PLAR-2ILSFN	328.2	366.6
PLAH-1ILSFN	326.2	361.9
PLAR-1LCh	330.8	365.6

PLAR-5LCh	316.7	360.5
PLAH-1LCh	326.8	365.2
PLAH-5LCh	322.7	361.2
PLAR-1HCh	304.9	352.7
PLAR-5HCh	313.2	357.0
PLAH-1HCh	318.8	359.1

3.2.3. Mechanical properties of the PLA based materials

The mechanical properties of the recycled plastics play a very important role in their possible applications in automotive, agriculture and packaging industries. The effect of the SFN and chitosan on the Vickers hardness of the recycled PLA was studied by means of microhardness measurements and the results are summarized in figure 6. It can be seen that the differences between the different samples are small. Nevertheless, there are some results that might be worth of interest. First of all, figure 6 shows that the different ageing processes and the reprocessing step caused a decrease on the hardness of PLA samples. This result can be attributed to the degradation of PLA, since the strength and rigidity of a polymer depend on its average molecular weight.

With respect to the effect of the different fillers, it can be seen that the addition of the silk fibroin nanoparticles results in a slight increase of the hardness of the materials. This result is especially striking for the PLAR-1HSFN sample, since the intrinsic viscosity results show that the presence of the nanoparticle led to some degradation of PLA. However, the increase of the hardness of the recycled PLA samples can be explained by the fact that SFN act as a reinforcement of the PLA matrix. Similar findings were reported by Patwa et al. (Patwa et al., 2018), who observed an increase of the elastic modulus, tensile strength, toughness and Shore D hardness in nanocomposites of virgin PLA with up to 2% of SFN.

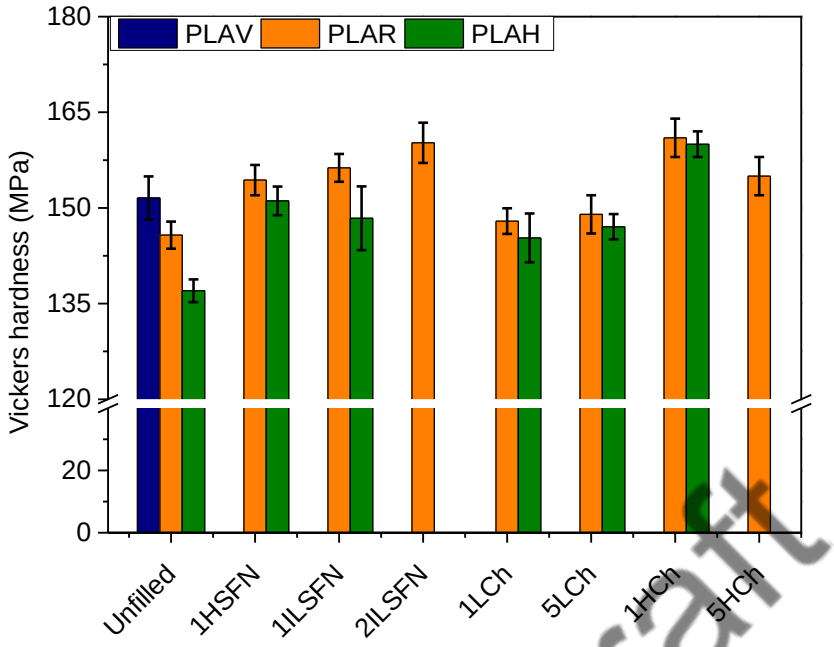

Figure 6. Vickers hardness of the PLA based materials.

In the case of the chitosan filled samples, it can be seen that the addition of chitosan has a small effect on the Vickers hardness, despite of the degradation observed in the samples of post-consumer PLA and high molecular weight chitosan. This behavior suggests that chitosan, especially that of high molecular weight, have 2 counteracting effects on the hardness of PLA. On the one hand, the degradation caused by chitosan should lead to a decrease of the hardness of the material. On the other hand, chitosan particles seem to have a reinforcement effect, increasing the hardness and counteracting the negative effect of the degradation. The overall result of these counteracting effects is that no important changes are observed in the hardness of the polymer.

3.2.4. Gas barrier properties of the PLA based materials

In the field of packaging applications, especially in that of food products, the gas barrier properties play a very important role. Hence, it is crucial to study the effect of the different organic fillers on the gas barrier properties of mechanical recycled PLA. Figures 7 and 8 present the results obtained for the permeability against O_2 and the water vapor transmission rate, respectively.

As it can be observed in figure 7, recycling does not seem to have a significant effect on the permeability coefficient of oxygen, despite the reduction of the intrinsic viscosity. Similar results were reported in a previous study, and were attributed to the dependence of the permeability on two parameters, namely the gas solubility and the diffusion coefficient (Beltrán et al., 2018b). These parameters are affected by the free volume and structure of the polymer, the size and chemical nature of the gas molecules and temperature. Mechanical degradation could lead to a decrease of the diffusion

coefficient, since shorter polymer chains can rearrange themselves better, reducing the free volume inside the polymer. On the contrary, the ageing, washing and reprocessing steps lead to an increase of the -COOH and -OH terminal groups, which could increase the affinity between the polymer and the gas molecules, increasing the solubility (Choudalakis and Gotsis, 2009). The presence of these two counteracting effects results in the small difference between PLAV and PLAR observed in figure 7.

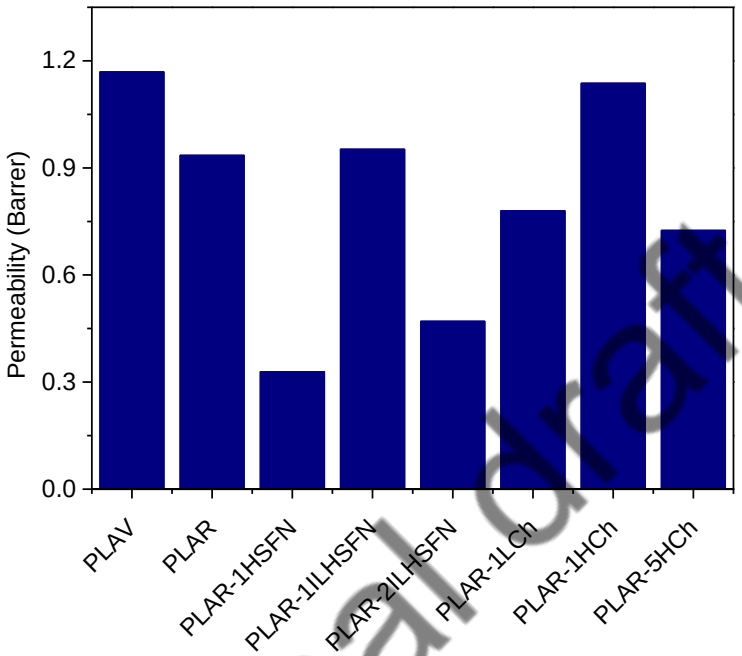

Figure 7. Oxygen permeability of PLA based materials.

Figure 7 reveals some noteworthy results regarding the effect of the fibroin nanoparticles. Firstly, it can be seen that the addition of HSFN leads to the reduction of the permeability coefficient of O_2, despite the degradation caused by this filler. This result could be attributed to the barrier effect of the nanoparticles dispersed in the polymer matrix, which increase the tortuosity of the diffusion path followed by the gas molecules and decrease the permeability of the material. In the case of the samples with ILSFN, a larger concentration of nanoparticles was needed to obtain a reduction of the permeability. This behavior could be explained by the worst interaction between ILSFN and PLA, observed in SEM microscopy. The poorer dispersion of the ILSFN reduces the barrier effect of the nanoparticles, making necessary to add more nanoparticles to decrease the permeability.

As for PLA-chitosan samples, the effect of the filler depends on the molecular weight of the chitosan. In the samples with low molecular weight chitosan, small amounts of the filler lead to a slight decrease of the permeability, probably due to the increase of the viscosity and subsequent reduction of the free volume in the material. However, it is worth to note that the PLAR with 5% low molecular weight chitosan presented a permeability coefficient over 7 Barrer (not shown in Figure 7). This behavior is probably due to the poor dispersion of the low molecular weight chitosan particles in the PLA

matrix. Meanwhile, the samples containing high molecular weight chitosan show a more moderated effect, despite the decrease observed in the intrinsic viscosity. This result might be an indicative of two counteracting effects of the addition of chitosan. On the one hand, the degradation of PLA leads to a larger free volume and thus an increased permeability. On the other hand, high molecular weight chitosan particles have a barrier effect, hindering the gas diffusion through the plastic.

Figure 8 summarizes the results obtained for the WVTR of the different PLA based materials. For the unfilled materials, it can be seen that the water vapor transmission rate slightly increases in PLAR and, especially, in PLAH. This behavior might be explained by the presence of a larger amount of terminal -COOH and -OH groups in the recycled materials, which increase the interactions with the water. Such increase in the interactions also increase the diffusion of the water vapor through the polymer films.

With regard to the effect of the silk fibroin nanoparticles, figure 8 shows that both HSFN and ILSFN are able to reduce the WVTR of recycled PLA, reaching values even lower than that of PLAV. As it was the case in the O_2 permeability, the reduction of the WVTR is due to the increase of the tortuosity of the diffusion path as a result of the dispersion of the nanoparticles in the polymer matrix. It is important to point out that a greater amount of ILSFN is needed to decrease the WVTR due to the aforementioned lower PLA-ILSFN interactions and overall poorer dispersion of ILSFN.

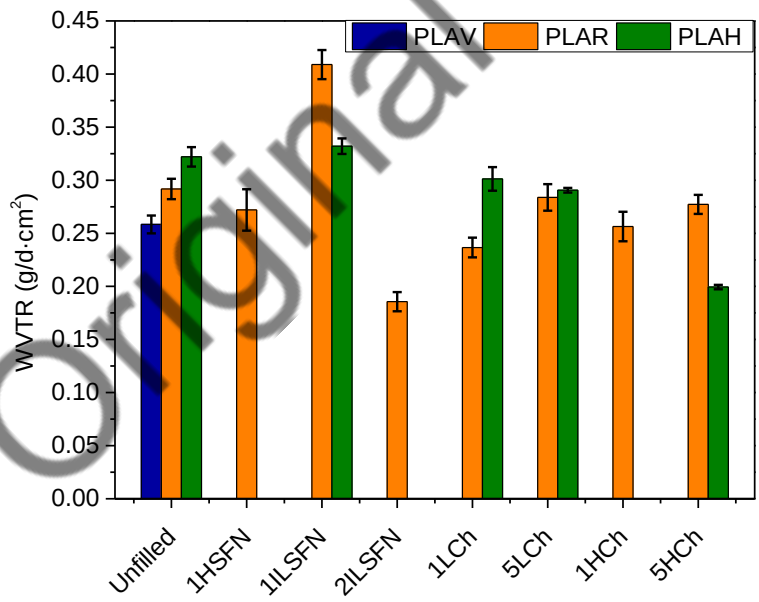

Figure 8. WVTR of the PLA based materials.

As far as the samples with chitosan are concerned, it can be seen on figure 8 that the effect of both low molecular weight and high molecular weight chitosan is small. This result might seem rather surprising, since it is expected that the WVTR of the PLA-chitosan samples to increase, due to the hydrophilicity of the chitosan (Bonilla et al., 2013). However, the obtained results agree with those of O_2 permeability, indicating that the dispersed chitosan phase has certain barrier effect, slowing down the diffusion

through the polymer films. In the conditions used in this study, the barrier effect seems to prevail over the hydrophilicity of chitosan, resulting in a slight decrease of WVTR in the PLA-chitosan samples.

Overall, the obtained results indicate that the addition of organic fillers results in a mechanically recycled PLA with improved properties. These results suggest that organic fillers are interesting alternatives for upgrading mechanically recycled PLA due to their availability and their renewable origin, which should contribute to lowering the environmental impact of using PLA. However, especial attention should be paid to the nature and amount of filler employed, since some properties could be negatively affected.

4. Conclusions

The effect of adding silk fibroin nanoparticles and chitosan on key properties in packaging applications of recycled PLA was studied. Neat PLA was subjected to two different ageing protocols and then melt reprocessed in conjunction with silk fibroin nanoparticles, prepared by two different methods, and chitosan of low and high molecular weight. As it was expected, the different ageing protocols along with the degradation suffered during the melt reprocessing led to a decrease of the intrinsic viscosity, Vickers hardness, thermal stability and an increase in the permeability of the recycled polymer. The results show that, overall, a good dispersion of the different fillers in polymer matrix was achieved. However, the effect on the viscosity varies with the kind on filler used and degradation level of PLA. In recycled PLA obtained from slightly degraded PLA, the addition of fibroin obtained by acid hydrolysis and high molecular weight chitosan led to some degradation of the polymer, while in the recycled PLA obtained from severely hydrolyzed plastic the intrinsic viscosity increased with all the fillers. Despite the degradation of PLA, both silk fibroin nanoparticles and, to a lesser extent, chitosan have a reinforcing effect on mechanically recycled PLA. The addition of carefully selected organic fillers led to an improvement of the thermal stability, mechanical properties and especially the barrier properties, which are key for packaging applications.

The addition of these organic fillers represents a potential cost-effective and environmentally sound method for improving the properties of mechanically recycled PLA, which might favor its recyclability, allowing to reduce the consumption of raw materials and contribute to a circular economy approach.

5. References

Auras, R., Lim, L., Selke, S.E.M., Tsuji, H., 2010. Poly(Lactic Acid): Synthesis, Structures, Properties, Processing, and Applications. John Wiley & Sons, New Jersey

Beltrán, F.R., Ortega, E., Solvoll, A.M., Lorenzo, V., de la Orden, M.U., Martínez Urreaga, J., 2018a. Effects of Aging and Different Mechanical Recycling Processes on the Structure and Properties of Poly(lactic acid)-clay Nanocomposites. J. Polym. Environ. 26, 2142-2152

Beltrán, F.R., Lorenzo, V., Acosta, J., de la Orden, M.U., Martínez Urreaga, J., 2018b. Effect of simulated mechanical recycling processes on the structure and properties of poly(lactic acid). J. Environ. Manag. 216, 25-31

Beltrán, F.R., Lorenzo, V., de la Orden, M.U., Martínez-Urreaga, J., 2016. Effect of different mechanical recycling processes on the hydrolytic degradation of poly(l-lactic acid). Polym. Degrad. Stab. 133, 339-348

Beltrán, F.R., de la Orden, M.U., Martínez Urreaga, J., 2018c. Amino-Modified Halloysite Nanotubes to Reduce Polymer Degradation and Improve the Performance of Mechanically Recycled Poly(lactic acid). J. Polym. Environ. 26, 4046-4055

Beltrán, F.R., Infante, C., de la Orden, M.U., Martínez Urreaga, J., 2019. Mechanical recycling of poly(lactic acid): evaluation of a chain extender and a peroxide as additives for upgrading the recycled plastic. J. Clean. Prod. 219, 46-56https://doi.org/10.1016/j.jclepro.2019.01.206

Bonilla, J., Fortunati, E., Vargas, M., Chiralt, A., Kenny, J.M., 2013. Effects of chitosan on the physicochemical and antimicrobial properties of PLA films. Journal of Food Engineering119, 236-243

Castro-Aguirre, E., Iñiguez-Franco, F., Samsudin, H., Fang, X., Auras, R., 2016. Poly(lactic acid)—Mass production, processing, industrial applications, and end of life. Adv. Drug Deliv. Rev. 107, 333-366

Cecchi, T., Giuliani, A., Iacopini, F., Santulli, C., Sarasini, F., TirillÃ², J., 2019. Unprecedented high percentage of food waste powder filler in poly lactic acid green composites: synthesis, characterization, and volatile profile. Environmental Science and Pollution Research 26, 7263-7271

Chinthapalli, R., Skoczinski, P., Carus, M., Baltus, W., de Guzman, D., Käb, H., Raschka, A., Ravenstijn, J., 2019. Bio-based Building Blocks and Polymers – Global Capacities, Production and Trends 2018 – 2023. nova-Institut GmbH, Germany

Choudalakis, G., Gotsis, A.D., 2009. Permeability of polymer/clay nanocomposites: A review. Eur. Polym. J. 45, 967-984

Cuadri, A.A., Martín-Alfonso, J.E., 2018. Thermal, thermo-oxidative and thermomechanical degradation of PLA: A comparative study based on rheological, chemical and thermal properties. Polym. Degrad. Stab. 150, 37-45

Di Lorenzo, M.L., 2006. Calorimetric analysis of the multiple melting behavior of poly(L-lactic acid). J. Appl. Polym. Sci. 100, 3145-3151

Elsawy, M.A., Kim, K., Park, J., Deep, A., 2017. Hydrolytic degradation of polylactic acid (PLA) and its composites. Renewable and Sustainable Energy Reviews79, 1346-1352

Elsawy, M.A., Saad, G.R., Sayed, A.M., 2016. Mechanical, thermal, and dielectric properties of poly(lactic acid)/chitosan nanocomposites. Polym. Eng. Sci. 56, 987-994

Farah, S., Anderson, D.G., Langer, R., 2016. Physical and mechanical properties of PLA, and their functions in widespread applications — A comprehensive review. Adv. Drug Deliv. Rev. 107, 367-392

Haider, T., Völker, C., Kramm, J., Landfester, K., Wurm, F.R., 2018. Plastics of the future? The impact of biodegradable polymers on the environment and on society. Angew. Chem. Int. Ed. 010.1002/anie.201805766

Hijazi, N., Le Moigne, N., Rodier, E., Sauceau, M., Vincent, T., Benezet, J., Fages, J., 2019. Biocomposite films based on poly(lactic acid) and chitosan nanoparticles: Elaboration, microstructural and thermal characterization. Polym. Eng. Sci. 59, E350-E360

Li, W., Sun, Q., Mu, B., Luo, G., Xu, H., Yang, Y., 2019. Poly(l-lactic acid) bio-composites reinforced by oligo(d-lactic acid) grafted chitosan for simultaneously improved ductility, strength and modulus. International Journal of Biological Macromolecules131, 495-504

Lozano-Pérez, A.A., Montalbán, M.G., Aznar-Cervantes, S., Cragnolini, F., Cenis, J.L., Víllora, G., 2015. Production of silk fibroin nanoparticles using ionic liquids and high-power ultrasounds. J Appl Polym Sci 132

Mülhaupt, R., 2013. Green Polymer Chemistry and Bio-based Plastics: Dreams and Reality. Macromol. Chem. Phys. 214, 159-174

Nagarajan, V., Mohanty, A.K., Misra, M., 2016. Perspective on Polylactic Acid (PLA) based Sustainable Materials for Durable Applications: Focus on Toughness and Heat Resistance. ACS Sustainable Chem. Eng. 4, 2899-2916

Niaounakis, M., 2019. Recycling of biopolymers – The patent perspective. European Polymer Journal114, 464-475

Patwa, R., Kumar, A., Katiyar, V., 2018. Effect of silk nano-disc dispersion on mechanical, thermal, and barrier properties of poly(lactic acid) based bionanocomposites. J Appl Polym Sci 135, 46671

Reddy, M.M., Vivekanandhan, S., Misra, M., Bhatia, S.K., Mohanty, A.K., 2013. Biobased plastics and bionanocomposites: Current status and future opportunities. Prog. Polym. Sci. 38, 1653-1689

Rossi, V., Cleeve-Edwards, N., Lundquist, L., Schenker, U., Dubois, C., Humbert, S., Jolliet, O., 2015. Life cycle assessment of end-of-life options for two biodegradable packaging materials: sound application of the European waste hierarchy. J. Clean. Prod. 86, 132-145

Soroudi, A., Jakubowicz, I., 2013. Recycling of bioplastics, their blends and biocomposites: A review. Eur. Polym. J. 49, 2839-2858

Suyatma, N.E., Copinet, A., Tighzert, L., Coma, V., 2004. Mechanical and Barrier Properties of Biodegradable Films Made from Chitosan and Poly (Lactic Acid) Blends. Journal of Polymers and the Environment 12, 1-6

Tao, Y., Xu, W., Yan, Y., Cao, Y., 2012. Preparation and characterization of silk fibroin nanocrystals. Polym. Int. 61, 760-767

Tesfaye, M., Patwa, R., Gupta, A., Kashyap, M.J., Katiyar, V., 2017. Recycling of poly (lactic acid)/silk based bionanocomposites films and its influence on thermal stability, crystallization kinetics, solution and melt rheology. International Journal of Biological Macromolecules101, 580-594

Zhao, P., Rao, C., Gu, F., Sharmin, N., Fu, J., 2018. Close-looped recycling of polylactic acid used in 3D printing: An experimental investigation and life cycle assessment. J. Clean. Prod. 197, 1046-1055

.